

## Regeneration of Model Supported Metal Catalysts

RONA GOLLOB<sup>1</sup> AND DADY B. DADYBURJOR<sup>2</sup>

*Department of Chemical Engineering and Environmental Engineering, Rensselaer Polytechnic Institute, Troy, New York 12181*

Received August 1, 1980; revised December 10, 1980

Regeneration of a model catalyst of Pt over  $\gamma$ -Al<sub>2</sub>O<sub>3</sub> was studied as a function of time using a TEM. The decrease in particle diameter was accomplished by heating the sample in air at 500°C for times up to 2 h. The results were analyzed using a model which is shown to be particularly valid for short times and large particle sizes. The model postulates a surface layer of oxide on the supported metal particle. The difference between Pt-Pt distances in the surface layer of platinum oxide and in the unoxidized metal gives rise to forces which may crack and split the particle. The experimental results indicate that the initial regeneration rate is rapid, and that the rate falls off after about 2 h of heating. Applying the model to the experimental data yields values for an average rate of oxidation of 2.37 nm/h, and a minimum particle diameter for crack initiation of 8.6 nm. These values are consistent with numbers obtained for these parameters from completely different circumstances.

### 1. INTRODUCTION

Alumina-supported platinum catalyzes reactions of dehydrogenation, isomerization, and hydrocracking of hydrocarbons. The deactivation of supported metal catalysts can occur by sintering, coking, and/or poisoning. Since platinum catalysts are expensive to manufacture, methods are needed for the "aged" catalyst to recover its original activity, i.e., for the "rejuvenation" of the catalyst. The process of present interest is one which regenerates a sintered supported metal catalyst.

That the oxygen content and the temperature of the gas phase surrounding the catalyst play important parts in the regeneration of sintered supported metal catalysts has been surmised for many years; however, the exact roles they play are still not well known. The objectives of this study are twofold: first to obtain transmission electron microscope (TEM) data on the time dependence of regeneration of a model supported metal catalyst, and second to

relate the kinetic data to a physical model of the regeneration process.

Adler and Keavney (1) reactivated aged catalysts by heating to 620°C in a static 60-psig O<sub>2</sub> atmosphere for 2 h. They felt that the apparent decrease in platinum size after reactivation is due to a disruption of the platinum lattice by oxygen atoms. They hypothesized that the oxygen atoms removed by subsequent hydrogen dosing leave fissures in the sintered particles, and these fissures are responsible for the increase in platinum surface area.

Johnson and Keith (2) found that regeneration occurs when the sintered catalyst is heated in dry air at 510–580°C followed by a reduction in hydrogen. They felt that an oxide of platinum would form in the presence of an oxygen atmosphere, and this compound would be stabilized by complexing with alumina (PtO<sub>2</sub> · alumina). The formation of the complex would then be responsible for the high dispersion of platinum that is found to occur.

Fiedorow and Wanke (3) used hydrogen chemisorption to characterize the dispersion of platinum on a support when the catalyst was exposed to oxygen isothermally in the range 500–700°C for various

<sup>1</sup> Current address: Combustion Engineering, Department 9487-423, Windsor, Conn. 06097.

<sup>2</sup> To whom correspondence should be addressed.

times. On heating the samples for 1 h, the dispersion first increases and then decreases as a function of temperature, with the maximum occurring around 550°C. Heating for 16 h does not change the dispersion further at temperatures where the dispersion increases with temperature after 1 h. At temperatures higher than the optimum temperature, however, the decrease in dispersion from the maximum value is much greater for the higher time period. Fiedorow and Wanke hypothesized that the increasing dispersion occurs because the net direction of molecular migration of platinum oxide (assumed to be PtO<sub>2</sub>) is from the crystallite phase to a monomolecular phase. Similarly, decreasing dispersion would be due to a net motion of molecules in the opposite direction.

Ruckenstein and Malhotra (4) observed changes in the average particle size using the TEM. On heating a model catalyst in air for 24 h at various temperatures, they observed a dramatic decrease in the size at 500°C, whereas at 600°C the particle size increases. There is also an increase in size at 400°C. They postulated qualitatively that the formation of the complex induces in the crystallite a strain which is relaxed by the fracture of the crystallite.

After the start of the present study, Stulga *et al.* (5) published the results of an attempt to duplicate the work of Ruckenstein and Malhotra described above. They were unable to obtain the dramatic decrease in particle sizes of Ref. (4), and concluded that molecular migration alone must be responsible for regeneration.

The present study differs from Refs. (4, 5) in that average particle sizes are obtained at several times during the regeneration process. Further, the time intervals used are relatively small, approximately 15 min. Preliminary data indicated that regeneration was negligible after about 2 h, and hence the runs were stopped at that time. In Refs. (4, 5), only two sets of data points were taken per run, one at the beginning and the other after 18 to 24 h. Details of our

experiment are given in Section 2. Our results show that there are changes in the average particle size with time. Although the changes are somewhat less than those of Ref. (4), they are definitely significant in a statistical sense. Duplicate measurements, on the other hand, show statistically insignificant changes from those on physically different samples regenerated for the same amount of time. In Section 3 is described a theoretical analysis which is particularly valid for large particle sizes and small regeneration times. The analysis is used in Section 4 to evaluate the present data and allows us to suggest possible reasons for the observed differences between the results of Refs. (4, 5) and the present study in Section 5.

## 2. EXPERIMENTAL

In general the method of Ruckenstein and Malhotra (4) was followed. Better than 99% pure thin aluminum foil was obtained from the Alpha Ventron Company. Small pieces of the foil (approximately 50 × 75 mm) were polished in an acid solution at 80°C for 150–180 s. The polishing solution contained 100 ml of 85% weight orthophosphoric acid, 4 ml of 70.4% weight nitric acid, and 20 ml of distilled water. The polished foil was washed in distilled water and dried in a desiccator for approximately 24 h. Aluminum oxide was prepared by anodization of the polished foil. The anodizing solution consisted of 150 ml of distilled water and 4.5 g of tartaric acid. The pH of the solution was adjusted to 5.5 by the addition of ammonium hydroxide. The distance between the cathode (stainless-steel rod) and the anode (aluminum foil) was approximately 20 mm. Since there was an initial surge of current during the anodization, a variable resistor was used to maintain a constant voltage of 20 V for 50 s. The foil was then washed in distilled water and transferred to a quartz crucible. The crucible and contents were heated in a 605°C muffle furnace for 20 h to ensure complete

transformation of the aluminum oxide to stable  $\gamma$ -alumina.

Platinum was deposited on the oxide films by use of a Commonwealth Scientific Corporation Mini-Coater. The Mini-Coater is a small dc glow discharge sputtering system. Argon gas was used in the chamber to avoid oxidation of the metal during sputtering. Platinum particles were obtained by using a current of 5–10 mA for about 30 s. At this point, some samples were prepared (as described below) for examination under the TEM. The remaining samples were calcined at 605°C in air for 24 h, to sinter the platinum islands, and then cooled to room temperature. A portion of these samples were examined under the TEM at this point. These samples will be termed sintered model catalysts.

The remaining samples were heated in the muffle furnace at 506°C, at which temperature regeneration was hypothesized to occur. The samples were removed from the furnace at various times, cooled to room temperature, and prepared for examination under the TEM. These samples will be termed regenerated model catalysts, and the time they were in the furnace at 506° is the regeneration time.

Preparation for TEM examination involved stripping the platinum/alumina film from the aluminum metal and mounting this film on grids. The films, about 300 Å thick, were then picked up on copper electron microscope grids. After drying, they were placed in the TEM for the determination of crystallite size.

Transmission electron micrographs of samples obtained as shown above were analyzed to obtain size distributions and surface-area-averaged diameters of the supported crystallites. In many cases micrographs were analyzed from different grids containing different portions of film floated off the same sample.

A preliminary set of regeneration experiments was run at 506°C, during which regeneration time was increased in 2-h increments. Analysis of the micrographs

showed a decrease in the average particle size, but the change occurred primarily within the first time increment. Consequently in the remaining experiments, the time increments were limited to approximately 0.25 h, and the maximum regeneration time to approximately 2 h.

Table 1 summarizes the data in terms of the surface-area-averaged diameter of the particles as a function of the time and temperature of treatment. The average diameter decreases up to a point, and then levels off.

Figure 1 is a micrograph representing a sample of the sintered model catalyst. Figures 2 and 3 are two of the micrographs cited in Table 1 representing regenerated catalyst. The regeneration times are 1 and 1.99 h, respectively. Histograms corresponding to Figs. 1 through 3 are shown in Figs. 4 through 6.

TABLE 1

Regeneration time (h)	Surface area averaged diameter (nm)	Histograms correspond to figure
<sup>a</sup>	8.2	
0 <sup>b</sup>	13.0 13.5	1,4
0.30	12.5	
0.77	11.3	
1.00	10.2 10.2 <sup>c</sup>	2,5
1.25	9.4 9.4 <sup>d</sup>	
1.50	9.0 8.9 <sup>d</sup>	
1.99	8.6	3,6
2.25	8.6	

<sup>a</sup> Fresh model catalyst.

<sup>b</sup> Sintered model catalyst.

<sup>c</sup> Same micrograph, twice the number of particles analyzed.

<sup>d</sup> Different micrograph of separate grids from the same sample.

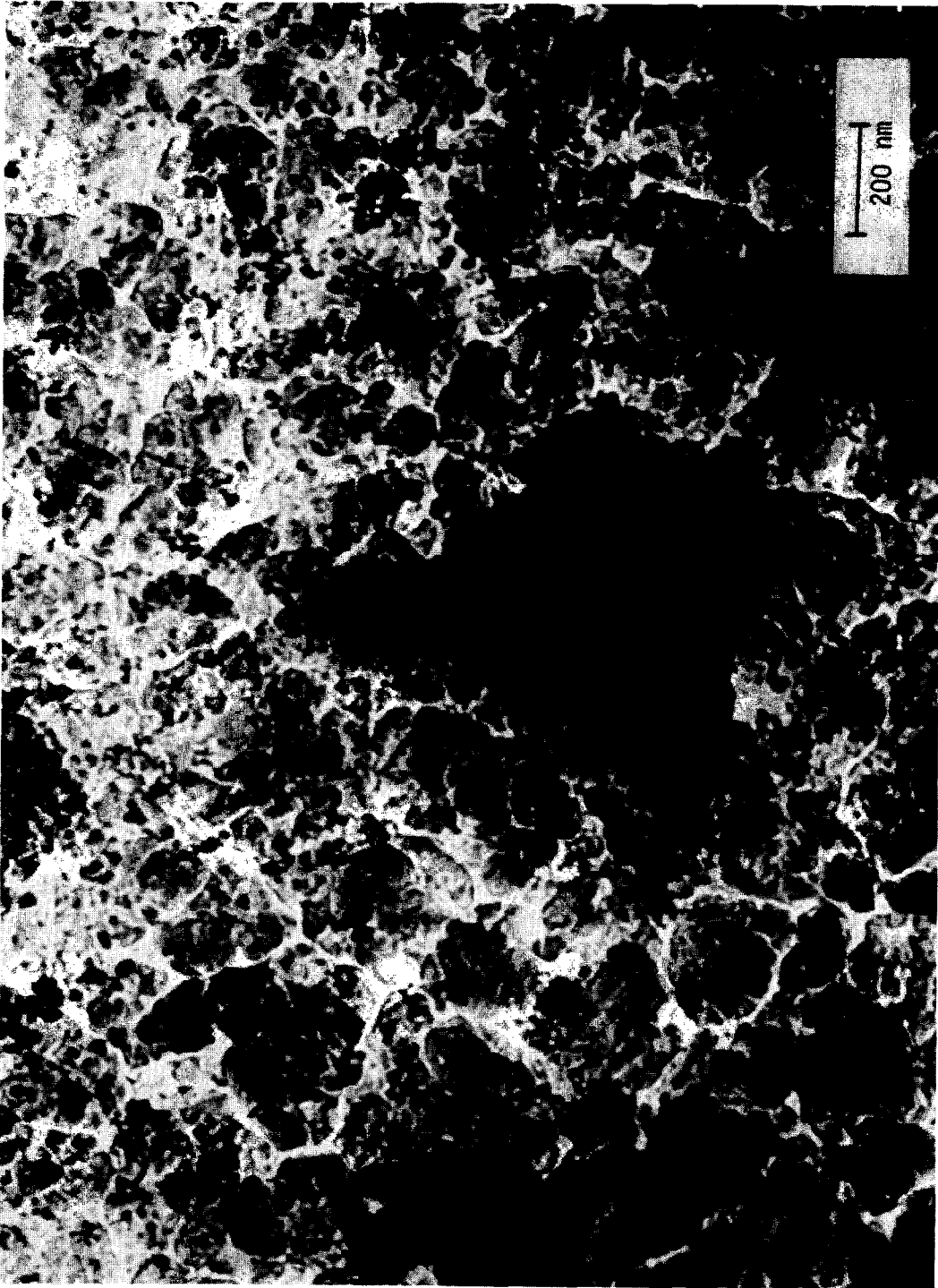


FIG. 1. Transmission electron micrograph of a sintered model catalyst resulting when the fresh model catalyst is heated in a 605°C furnace for 20 h and subsequently cooled.



Fig. 2. Micrograph of the sintered catalyst regenerated for 1 h at 506°C.

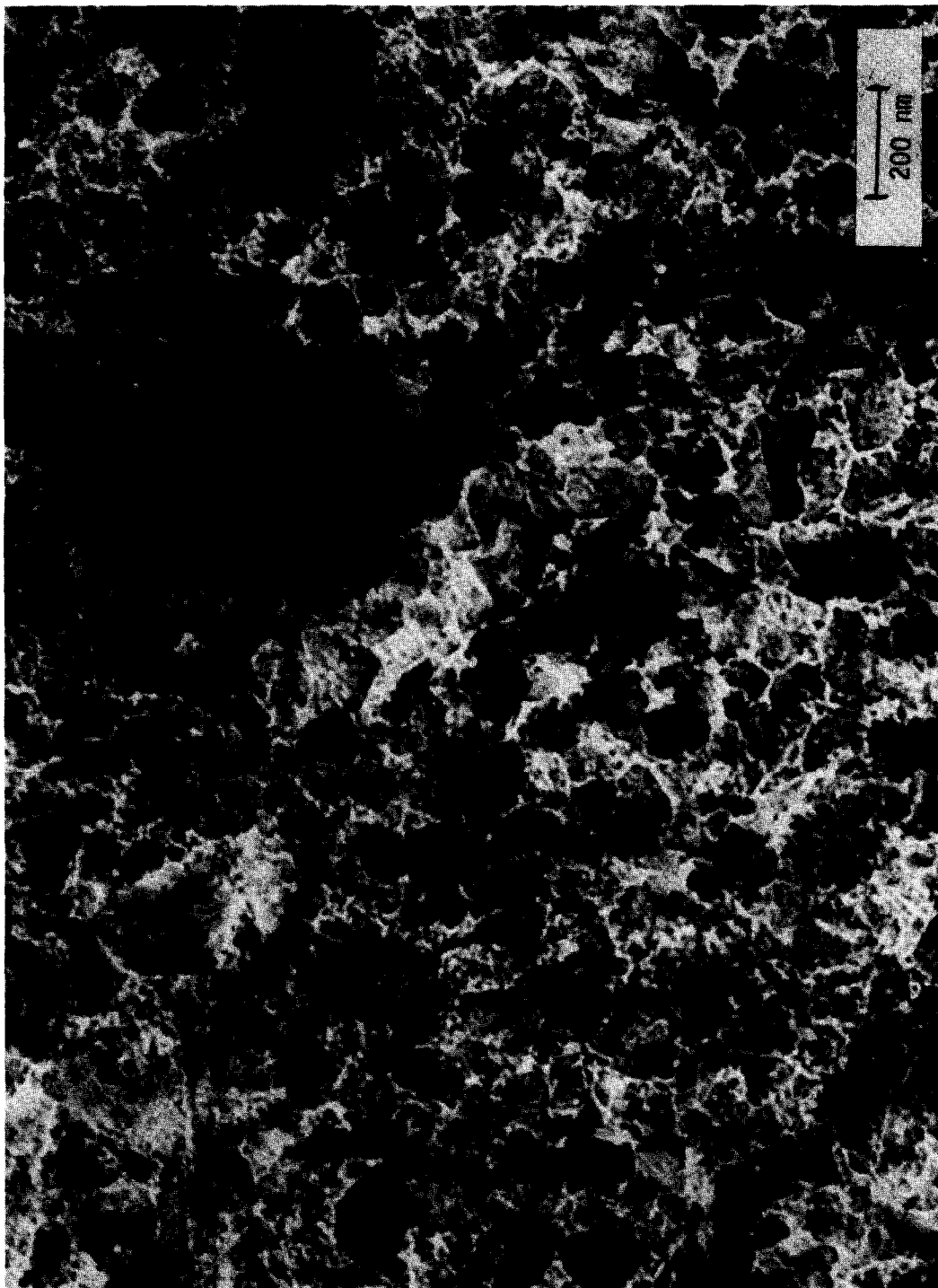


FIG. 3. Micrograph of the sintered catalyst regenerated for 1.99 h at 506°C.

It is of interest to compare pairs of samples removed from the oven at the same time, to see if the differences between such size distributions are significant or if they can be ascribed to random differences. This is done by using the so-called  $t$  test. Where the variances of the two particle size distributions are not too different, and where the same number of particles are counted in both samples, the parameter  $t$  can be calculated by using the relation

$$t = (\mu_A - \mu_B) / \{(\sigma_A^2 + \sigma_B^2)/n\}^{1/2},$$

where subscripts A and B denote the two samples,  $\mu_i$  and  $\sigma_i^2$  are the mean and variance of the particle size distribution of sample I, and  $n$  is the number of particles in each sample. The calculated values of  $t$  can then be compared with values corresponding to probabilities that the difference between the samples is random. The calculated values of  $t$  for sample pairs at regeneration times of 0, 1.0, 1.25, and 1.5 h are shown in Table 2. Shown for comparison are values of  $t$  corresponding to 0.1, 5, and 90% probabilities that the differences are random. For sample pairs at

the same regeneration times, the differences in average size are clearly random.

Also shown in Table 2 are values of  $t$  for pairs of samples at different regeneration times. Even if the samples differ in regeneration times by small amounts, 15 to 20 min, the probability that the average diameters are only randomly different is less than 5% in almost all the cases considered. About the only exceptions are the pair of samples at 0 and 0.3 h regeneration time, i.e., at the start, and the pair at 1.99 and 2.25 h regeneration time, i.e., at the end. We show later that these exceptions are to be expected.

When the samples differ in regeneration times by approximately 1 h or greater, the probability that the differences are random drops to less than 0.1%. This is also shown in Table 2.

Hence while samples removed after the same regeneration time are statistically similar, the differences between samples removed 15 min or more apart are statistically significant.

A mass balance shows that the fractional change in total surface area can be related to the fractional change in the average diameter by

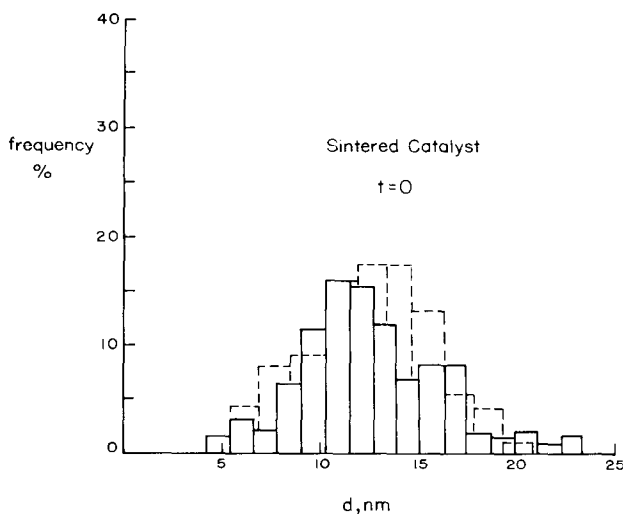


FIG. 4. Histogram from Fig. 1.

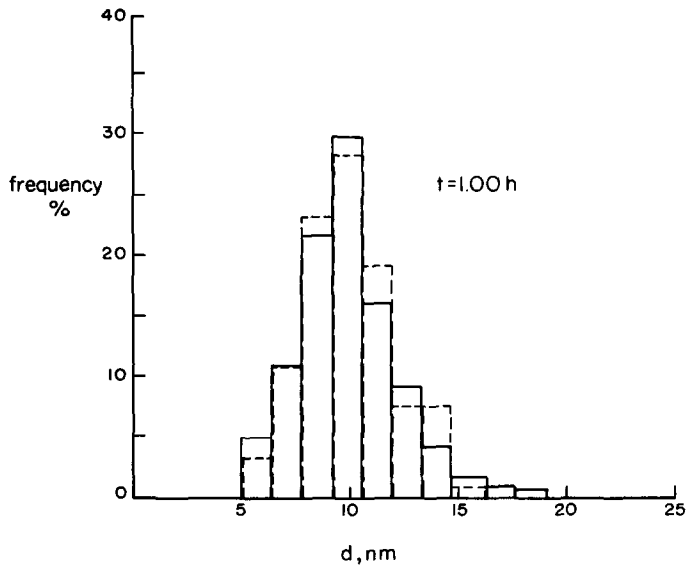


FIG. 5. Histogram from Fig. 2.

$$\frac{S(t)}{S(0)} = \frac{\bar{d}(0)}{\bar{d}(t)} \quad (1)$$

## 3. THEORY

and the points of Fig. 7 represent all of the experimental data plotted on this basis. The data are analyzed in the following section.

Many analyses of regeneration phenomena use what can be termed, in a formal sense, the "thermodynamic" approach. Here complete, or nearly complete, forma-

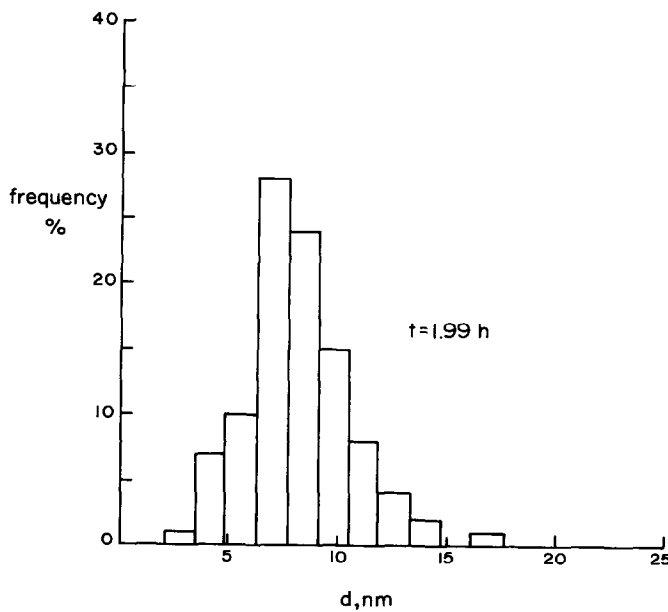


FIG. 6. Histogram from Fig. 3.



TABLE 2  
Values of  $t$  Calculated for Pairs of Samples at the Same or Different Regeneration Times,  $t$

Regeneration time (h)		$t$ (h)
Sample A	Sample B	
0	0	0.372
1.0	1.0	0.021
1.25	1.25	0.773
1.50	1.50	0.763
0	0.3	1.673
0.30	0.75	3.519
0.77	1.0	3.520
1.0	1.25	3.331
1.25	1.50	1.213
1.50	1.99	2.316
1.99	2.25	0.105
0.30	1.0	6.856
1.0	1.99	6.896
0.30	1.99	13.381

Note. The value of  $t$  corresponding to a 90% probability of random differences is 0.126 for  $n = 200$  particles counted. Similarly values of  $t$  for probabilities of 5 and 0.1% are 1.974 and 3.348, respectively.

tion of platinum oxide crystallites is implied, and the properties of this oxide are compared with those of the platinum crystallites. For instance, the "wetting" model, originally mentioned by Ruckenstein and Pulvermacher (6) and developed by Ruckenstein (7) and Ruckenstein and Chu (8), compares the ability of platinum oxide to

wet the alumina substrate with the wetting ability of platinum metal. The dispersion model, originated by Flynn and Wanke (9), developed by Fiedorow and Wanke (3), and quantified by Yao and co-workers (see, for example, (10)), compares the two-dimensional solubility of platinum oxide on the substrate with that of platinum crystallites.

An alternative approach, perhaps "kinetic" in a formal sense, requires only a layer of platinum oxide to be formed on the metal crystallite. The strain model compares the Pt-Pt distance in the oxide layer with the Pt-Pt distance that would exist in the unoxidized metal. When the resulting strain in the oxide generates a sufficiently large stress, a crack is initiated, which may result in the fracture of the crystallite. This approach was qualitatively suggested by Ruckenstein and Malhotra (4), and a quantitative analysis was developed by Dadyburjor (11). Direct observations of this phenomenon have been reported by Ruckenstein and Chu (8).

In comparing these two approaches, note (12) that the oxidation of platinum crystallites can be expected to take a finite amount of time. Hence, the thermodynamic approach models probably play a lesser role during short times of exposure to oxygen. Further the Gibbs-Thomson relationship implies that thermodynamic dispersion is much more rapid from smaller particles than from larger ones. Consequently the thermodynamic approach is probably most valid for relatively small particles at relatively large times, while the kinetic approach is valid for large particle sizes and short time periods. Since the latter set of criteria most closely fit the present conditions, only the strain model is used to analyze the experimental data of the previous sections. Further quantitative justification for this will be given during the development of the model and the evaluation of the data.

In this model, it is assumed that at time  $t$ , the platinum particles are hemispherical of

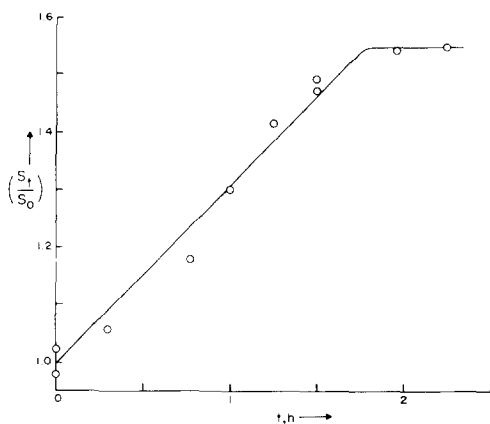


FIG. 7. Platinum surface area ( $S_t/S_0$ ) versus time.

average diameter  $d$ . Each particle contains an inner hemisphere of metal of diameter  $d_m$  and an outer shell of oxide of uniform thickness  $l$ . Assuming no plastic flow occurs, the overall particle diameter  $d (= d_m + 2l)$  remains constant during oxidation. Therefore, the force due to lattice mismatch is (11)

$$F_d = E(\Delta a/a_{pt}) \frac{\pi}{8} \{d^2 - (d - 2l)^2\}. \quad (2a)$$

Here  $a_{pt}$  is the Pt-Pt distance in the metal, and  $\Delta a$  is the difference between the Pt-Pt distance in the metal oxide and  $a_{pt}$ . Finally,  $E$  is the Young's modulus of the platinum oxide. The surface force is (11)

$$F_s = \sigma\pi(d/2), \quad (2b)$$

where  $\sigma$  is the surface tension of the platinum oxide. When the oxide thickness reaches a certain (critical) value, the difference between  $F_s$  and  $F_d$  is just equal to a "critical" force required for a crack to be initiated on the crystallite. In what follows we consider the critical force to be zero, i.e., the crack is initiated when  $F_s = F_d$ . Then the critical thickness of the oxide layer is

$$l_{crit} = \frac{d}{2} \left\{ 1 - \left[ 1 - \frac{4\sigma/E}{E(\Delta a/a_{pt})} \frac{1}{d} \right]^{1/2} \right\}. \quad (3)$$

A plot of  $l_{crit}$  vs  $d$  is shown in Fig. 8. The following asymptotes are noted. At large values of  $d$ ,  $l_{crit}$  is small and independent of  $d$ , i.e., only a relatively small layer of oxide need be formed on large crystallites before a crack is initiated, and the size is decreased by this phenomenon. Also, note that if the crystallite dimension is such that

$$d = 4(\sigma/E)/(\Delta a/a_{pt}),$$

then

$$l_{crit} = d/2.$$

This indicates that there is a minimum diameter for crack initiation, given by

$$d_{min} = 4(\sigma/E)/(\Delta a/a_{pt}). \quad (4a)$$

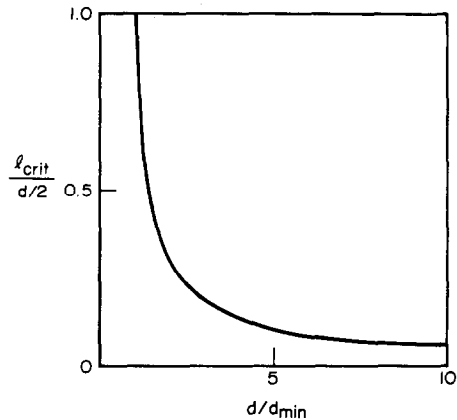


FIG. 8. Critical oxide thickness ( $l_{crit}$ ) versus diameter.

Crystallites smaller than  $d_{min}$  will not split, i.e., small particles will be completely converted to the oxide. Under these conditions, "thermodynamic" approaches alone will cause further decreases in particle size.

Following Ref. (11), the rate of change of surface area for a system of particles using the strain model only is

$$\frac{dS(t)}{dt} = \frac{0.26 r_0}{l_{crit}(\bar{d}(t)) - l'(\bar{d}(t))} S(t), \quad (4b)$$

where  $r_0$  is the rate of oxidation of platinum, assumed zeroth order in oxide thickness for the sake of simplicity. In the denominator,  $\bar{d}(t)$  is the average particle diameter of the system, and  $l_{crit}(d)$  is the critical thickness of the oxide layer for a particle of diameter  $d$  and can be obtained from Eq. (3). Finally,  $l'(\bar{d}(t))$  is the oxide thickness for a particle of diameter  $\bar{d}(t)$  immediately after the fracture of its parent particle.

Consider the situation when the average particle diameter is large. As shown earlier,  $l_{crit}(\bar{d}(t))$  is independent of  $d$  under these conditions. Clearly  $l'$  would also be size independent. From Eq. (1) this implies that  $l_{crit}$  and  $l'$  are independent of  $S(t)$ . Hence Eq. (4b) shows only a first-order dependence on surface area. This was the result obtained in Ref. (11).

In general the size dependence of  $l_{crit}$  and  $l'$  must be taken into account, and this is done as follows.

At  $t = 0$ , there is no oxide layer present on the metal particles. Consequently  $l' = 0$ , and the initial rate equation may be obtained by substituting Eq. (3) into (4) and grouping terms

$$\left(\frac{dx}{dt}\right)_0 = \frac{Kx^2}{1 - (1 - \delta x)^{1/2}} \quad (5a)$$

Here,

$$K \equiv 0.52 r_0/\bar{d}(0), \quad (6a)$$

$$x \equiv S(t)/S(0), \quad (6b)$$

and

$$\delta \equiv d_{min}/\bar{d}(0). \quad (6c)$$

Equation (5a) is valid for  $0 \leq t < t_0$ , where  $t_0$  is the time required to split a particle of diameter equal to the initial average diameter of the system. At this time, the value of  $x, x_0$  is

$$x(t = t_0) \equiv x_0 \equiv 2^{1/3} \quad (7a)$$

by geometry. We use Eq. (7a) below to determine  $t_0$ .

For time greater than  $t_0, l'$  can be shown by geometry to be

$$l'(\bar{d}) = 0.5^{1/3} l_{crit}(2^{1/3} \bar{d}), \quad (8)$$

where  $2^{1/3} \bar{d}$  is the diameter of the parent particle of the particle of size  $\bar{d}(t)$ . Substituting Eq. (8) in Eq. (4) and rearranging,

$$\frac{dx}{dt} = \frac{Kx^2}{(1 - 0.5^{1/3} \delta x)^{1/2} - (1 - \delta x)^{1/2}} \quad (5b)$$

This relation is valid in the region  $t_0 \leq t < t_\infty$ , where  $t_\infty$  is the time at which the average diameter equals  $d_{min}$ , the minimum value for crack initiation. The corresponding value for  $x$  is

$$x(t = t_\infty) \equiv x_\infty \equiv 1/\delta. \quad (7b)$$

For time greater than  $t_\infty$ , Eq. (3) is no longer valid and the rate of change of surface area by this phenomenon is zero, i.e.,

$$dx/dt = 0. \quad (5c)$$

Of course this is not to imply that no further change in surface area is possible, but rather that "thermodynamic"-type phenomena will predominate at times greater than  $t_\infty$ .

Solution of Eq. (5a) with initial condition  $x(t = 0) = 1$  yields the surface area-time relationship, in the region  $0 \leq t < t_0$ ,

$$f_1(\delta x) = t + f_1(\delta), \quad (9a)$$

where

$$f_1(y) = \frac{\delta}{K} \left\{ \frac{1}{2} \ln \left[ \frac{1 - (1 - y)^{1/2}}{1 + (1 - y)^{1/2}} \right] - \frac{1}{1 + (1 - y)^{1/2}} \right\}. \quad (9b)$$

From Eq. (7a),

$$t_0 = f_1(2^{1/3} \delta) - f_1(\delta). \quad (9c)$$

Similarly, from Eq. (5b) for  $t_0 \leq t < t_\infty$ , using Eq. (9c) for the initial condition, the surface area-time relationship is

$$f_1(\delta x) - 0.5^{1/3} f_1(0.5^{1/3} \delta x) = t - t_0 + f_1(2^{1/3} \delta) - 0.5^{1/3} f_1(\delta). \quad (10a)$$

From Eq. (7b),

$$t_\infty = t_0 + 0.5^{1/3} \{ f_1(\delta) - f_1(0.5^{1/3} \delta) \} - f_1(2^{1/3} \delta). \quad (10b)$$

The rate of change of surface area at large times ( $t > t_\infty$ ) is not considered here.

In the following section we use Eqs. (9) and (10) to evaluate the parameters of the regeneration process using the experimental data described earlier.

#### 4. RESULTS

The data gathered in Fig. 7 can now be analyzed. Note that after a regeneration time of approximately 2 h, the rate of increase in surface area drops off considerably. Hence the data gathered at shorter times can be analyzed using only the strain model. Recall that this approach is valid for large particle sizes and small times of regeneration.

Fitting these points to Eqs. (9a) and (10a) yields

$$K = 0.0929 \text{ h}^{-1}, \quad (11a)$$

$$\delta = 0.65, \quad (11b)$$

where these parameters are defined in Eqs. (6). From Eqs. (9b), (10b), and (11), values of the "initial" time  $t_0$  and "final" time  $t_\infty$  are

$$t_0 = 1.07 \text{ h}, \quad (12a)$$

$$t_\infty = 1.43 \text{ h} \quad (12b)$$

for this particular system. Note that  $t_\infty$  is less than the time at which the curve of Fig. 7 levels off. This is expected, and is discussed below. Values of  $d_{\min}$  and  $r_0$ , calculated from Eqs. (6) and (11) are

$$d_{\min} = 8.61 \text{ nm}, \quad (13a)$$

$$r_0 = 2.37 \text{ nm/h}. \quad (13b)$$

## 5. DISCUSSION

The theoretical model is actually a combination of three effects with the first effect occurring between  $t = 0$  and  $t = t_0$ , the time needed for the first split to occur. The second effect occurs between  $t = t_0$  and  $t = t_\infty$ , the time at which the final split takes place. Finally, for  $t > t_\infty$ , it is assumed that regeneration can occur by "thermodynamic"-type approaches only.

In this regard, recall that the probability of random occurrences accounting for differences in average particle size with time is greatest at the smallest time period (0–0.3 h) and between 1.99 and 2.25 h. The former case corresponds to the period before splitting commences. The latter case corresponds to the period after splitting ceases.

Note that the value of  $t_\infty$  is less than the value at which the regeneration curve levels off in Fig. 7. Part of this effect is tied to the use of an average diameter. This use ignores the fact that some particles are much larger than  $d_{\min}$  and may continue to split (and increase the surface area) even

when the average diameter is  $d_{\min}$  or less. More importantly, however, note that a particle of diameter  $d_{\min}$  can split, and would do so in the interval between  $t_\infty$  and the leveling-off time. The particles formed of course would not themselves decrease in size by this mechanism, since their diameters are less than  $d_{\min}$ .

As seen from Fig. 7, essentially complete regeneration of the aged catalyst occurs in less than 2 h at 506°C. This agrees with the results of Schwarzenbek and Turkevich (13) and Carballo and Wolf (14). The former work found that regeneration occurs in times from 15 min to 2 h at temperatures from 950 to 1150°F, with an oxygen partial pressure of about 14.7 psia. After pretreating the catalyst in oxygen at 360°C for 2 h, Carballo and Wolf (14) found that the activity in the catalyst was essentially the same as that of the fresh catalyst. It should be noted that the work of Refs. (13, 14) was performed in an oxygen atmosphere at high pressures, whereas in this study the catalysts were regenerated in air.

From the present model, and confirmed by the experimental results, the catalyst does not become completely restored to the fresh catalyst surface area. There is a slight loss in the catalytic activity for the regenerated catalyst versus a fresh catalyst (diameters of 8.61 nm versus 8.19 nm, respectively). As mentioned above, the catalyst of Carballo and Wolf (14) returned to its original activity. Kogler and Queck (15) found that the regenerated catalyst exhibited the same activity as that of the fresh catalyst in the conversion of cyclohexane to benzene. Schwarzenbek and Turkevich (13) reported that when the aged catalyst was treated with oxygen, the catalyst was restored to its original activity and substantially to its original selectivity. Also, Weidenback and Furst (16) found that the activity for the isomerization of *n*-hexane is essentially the same for fresh and regenerated catalysts.

It is of interest to compare the values of  $r_0$  and  $d_{\min}$  obtained by using the strain model for regeneration with values from

other situations. Berry (17) measured the rate of oxidation of platinum in resistance thermometers at 450°C. Although his growth curves are not linear, as assumed by us, an average growth rate of approximately 0.5 nm/h can be obtained from his results. Initial rates would be much higher. Krier and Jaffee (18) report rates that were measured at much higher temperatures. Extrapolating these to 500°C results in values of the order of 0.1 nm/h. Both numbers compare favorably with the value of  $r_0$  in Eq. (13b).

Since values of  $\sigma$  and  $E$  for platinum oxide are not available, it is assumed that the ratio of these quantities is approximately equal to that of platinum metal. The value of  $\Delta a$  is obtained using the structure obtained by Ducros and Merrill (19) for the oxide layer formed on platinum. With 0.304 nm for the Pt–Pt distance in the oxide,  $a_{Pt}$  set equal to 0.277 nm, and  $\sigma/E$  of the order of  $10^{-10}$  m (20) the value of  $d_{min}$  is of the order of 10 nm. This compares well with the value of  $d_{min}$  obtained from experimental regeneration data in Eq. (13a).

We cannot completely account for the differences between the present results and those of Ref. (5), where no significant changes in particle size were noted after 18 h. The present model suggests, however, that differences between the initial average particle size and the minimum diameter for crack propagation govern the particle splitting mechanism and the time at which this faster process is superseded by the slower thermodynamic mechanisms of redispersion.

## 6. CONCLUSIONS

A model platinum catalyst supported on alumina can be regenerated by heating the sintered catalyst at 500°C. The sintered catalyst was obtained by heating a fresh catalyst at 605°C for 24 h. The regenerated catalyst exhibited a decrease in platinum crystallite size, thus effecting an increase in platinum surface area.

The regeneration process was run up to 2 h. The initial decrease in crystallite size was very rapid, with the rate later decreasing. This is consistent with the strain model, where smaller particles require a greater critical thickness of the metal oxide to be formed before a crack can be initiated. The experimental results support the theory of the formation of a platinum–alumina complex at high temperatures.

The model determines values of  $t_0$  and  $t_\infty$  which are not inconsistent with values obtained for the regeneration of industrial catalysts.

The model also determines both the minimum diameter for crack initiation  $d_{min}$ , and the average rate of oxide formation,  $r_0$ . These values compare favorably with those obtained under considerably different circumstances. This lends further credence to the use of the strain model to describe regeneration of supported metal catalysts, at least for short regeneration times and larger particle sizes.

## REFERENCES

1. Adler, S. F., and Keavney, J. J., *J. Phys. Chem.* **64**, 208 (1960).
2. Johnson, M. F. L., and Keith, C. D., *J. Phys. Chem.* **67**, 200 (1963).
3. Fiedorow, R. M. J., and Wanke, S. E., *J. Catal.* **43**, 34 (1976).
4. Ruckenstein, E., and Malhotra, M. L., *J. Catal.* **41**, 303 (1976).
5. Stulga, J. E., Wynblatt, P., and Tien, J. K., *J. Catal.* **62**, 59 (1980).
6. Ruckenstein, E., and Pulvermacher, B., *J. Catal.* **29**, 224 (1973).
7. Ruckenstein, E., in "Growth and Properties of Metal Clusters" (J. Bourdon, Ed.). Elsevier, Amsterdam, 1980.
8. Ruckenstein, E., and Chu, Y. F., *J. Catal.* **59**, 109 (1979).
9. Flynn, P., and Wanke, S. E., *J. Catal.* **33**, 233 (1974).
10. Yao, H. C., Sieg, M., and Plummer, H. K., Jr., *J. Catal.* **59**, 365 (1979).
11. Dadyburjor, D. B., *J. Catal.* **57**, 504 (1979).
12. Dadyburjor, D. B., in "Catalyst Deactivation" (G. F. Froment and B. Delmon, Eds.). Elsevier, Amsterdam, 1980.

13. Schwarzenbek, E. F., and Turkevich, J., U.S. Pat. 3,400,073, Sept. 3, 1968.
14. Carballo, L. M., and Wolf, E. E., *J. Catal.* **53**, 366 (1978).
15. Kogler, H., and Queck, S., *Chem. Tech.* **14**, 541 (1962).
16. Weidenback, G., and Furst, H., *Chem. Tech.* **15**, 583 (1963).
17. Berry, R. J., *Surface Sci.* **76**, 415 (1978).
18. Krier, C. A., and Jaffee, R. I., *J. Less-Common Metals* **5**, 411 (1963).
19. Ducros, R., and Merrill, R. P., *Surface Sci.* **55**, 227 (1976).
20. Weast, R. C., Ed., "Handbook of Chemistry and Physics," 51st ed., Chemical Rubber Co., Cleveland, Oh., 1970.